Study on recycle of granulated blast-furnace slag as an adsorbent for ammonium remediation in wastewater

Trinh Minh Viet, Nguyen Tuan Minh[*], Nguyen Thi Phuong Thao, Phung Linh Phuong, Trinh Van Tuyen

Institute of Environmental Technology, Vietnam Academy of Science and Technology, 18 Hoang Quoc Viet, Cau Giay, Ha Noi, Viet Nam

[*]Email: *nguyentuanminh82@gmail.com*

Abstract. Blast-furnace slag (BFS) is enormously generated each year and has been considered as hazardous solid waste which is posing a significant pressure on waste treatment in terms of storage and transportation. This study aims to recycle BFS as a material for ammonium adsorption from an aqueous solution. Natural-state BFS and acidic-modified by using HNO_3 at various concentration of 0.5 M, 1 M, and 3 M (A-BFS1, A-BFS2, and A-BFS3) was examined. The surface characteristics of the materials were examined by BET analysis and Scanning Electron Microscope. The adsorption of ammonium on the BFS materials was conducted in batch mode at various conditions of contact time, pH level, adsorbent dosage, and initial concentration of ammonium. The results indicated that the HNO_3 modification exhibited pore creations and surface enhancement as the A-BFS3 has 25.7 times larger surface area and 10.3 times pore size improvement. The A-BFS3 showed good ammonium adsorption capacity compared to other materials, which is 1.81 mg/g at the optimum conditions of pH 6, contact time of 120 minutes, and dosage of 0.5 g in 50 mL of 20 mg/L ammonium solution. Langmuir and Freundlich adsorption isotherm models of the A-BFS3 material showed a relatively good correlation with R^2 values of 0.999 and 0.9625, respectively.

Keywords: blast-furnace slags, adsorption, ammonium, wastewater, acidic modification.

Classification numbers: 3.3.2, 3.4.2.

1. INTRODUCTION

Ammonium (NH_4^+) is one of the most common pollutants found in groundwater and wastewater. NH_4^+ comes from various sources from human, animal, certain fertilizers to even discharge from industrial, agricultural, and domestic activities [1]. The exceeded release of NH_4^+ in the water body exhibits eutrophication, and lethality to aquatic species. Exposure to a high concentration of ammonia may cause loss of equilibrium, convulsion, coma, or even death [2]. NH_4^+ presenting in drinking waters also leads to algae growth and bacterial population, metal pipe corrosion, and a higher requirement of chlorine added for disinfection by the formation of chloramines [3]. The criteria for the acceptable amount of NH_4^+/NH_3 in water is stringent in many countries. WHO guidelines have set the allowable concentration of NH_4^+ in drinking water

is under 1.5 mg/L, while the Vietnam National technical regulation on drinking water set the safe amount of NH_4^+ is not exceeding 3 mg/L [4, 5].

There are many approaches that have been studied and employed for the abatement of NH_4^+ in the wastewater, such are: biological treatment, chemical precipitation, air stripping, membrane filtration, and adsorption. Among these methods, adsorption draws the most attention due to its simplicity, economical and environmental friendly in terms of configuration and operation [6]. Halim *et al.* reported that the polar surface of adsorbent plays a crucial role in the adsorption of NH_4^+ since the high cation-exchange capacity materials such as zeolite and composite materials possessed higher NH_4^+ adsorption capacity than that of activated carbon [7]. The low-cost adsorbent which is derived from the by-product of agriculture and industrial activities has even drawn huge attention in terms of economical and environmental benefits [8]. Eleven agricultural residues were proven to be comparable to the mineral adsorbent in the study of Liu *et al.* [9]. Among other residues, the dry grounded leaves of Boston ivy, phoenix tree, sunflower tree, southern magnolia, loquat, and poplar achieved NH_4^+ adsorption capacity above 2.5 mg/g. Adsorbent modification is also a common technique to enhance the adsorption capacity by either enlarging the surface area and pore size or polarizing the surface group of the material. The popular method the oxidation of the material using acid [10, 11]. Results of Vassileva *et al.* showed that NH_4^+ adsorption capacity of activated carbon was improved from 11.57 mg/L to 28.42 mg/L after oxidation with nitric acid [10]. The adsorption capacity of saw-dust activated carbon reached 6 to 11 mg/g after modification with HNO_3 and Na_2CO_3 [11].

Among various type of industrial by-product, the slags from steel manufacture is the most generated in weight, which equivalent 30 % to 40 % the weight of produced steel. This number will upsurge in the near future as steel production is growing annually. Consequently, there is an indisputable pressure on the environmental and economical aspect since it takes up expensive costs on transportation and large land use for storage. Blast furnace slag (BFS) is a nonmetallic type of slag, which is generated from the blast furnace in form of a small granular with a diameter from 10 to 20 mm. The BFS mostly composed of metal oxide which has relatively good pore size and surface area. These characteristics exhibit the potential for BFS to be used as a material for adsorption. A few studies were conducted to examine the adsorption capacity of BFS toward metal ions such as Cu(II) and As(III) which showed promising results paving a way for future application [12 - 14]. However, further studies are needed to examine the adsorption capacity of BFS with other pollutants in water like NH_4^+ and the effect of modification on adsorption enhancement. Therefore, this study was conducted to assess the adsorption capacity of the BFS and acidic modified BFS toward NH_4^+. The natural-state BFS from Formorsa Ha Tinh Steel Corporation (Ha Tinh, Viet Nam) and its acidic modified with HNO_3 at different acid concentrations were compared in the batch adsorption experiments. The effects of various experimental conditions such as contact time, pH level, adsorbent dosage, and initial concentration on the NH_4^+ adsorption by the BFS material were also investigated.

2. MATERIALS AND METHODS

2.1. Materials

BFS was collected from Formosa Ha Tinh Steel Corporation, crushed, and sieved to the narrow particle size from 0.25 to 0.5 mm. The sieved material was then washed and dried in the oven for 2 hours at 105 ^{o}C (BFS). The acidic modified BFS was prepared by mixing the 25 g of the material with 100 mL of HNO_3 at different concentrations of 0.5 M (A-BFS1), 1 M (A-

BFS2), and 3M (A-BFS3) for 12 hours. The material then was washed with distilled water to pH 8, subsequently dried at 105 $^\circ$C for 2 hours to obtain the final modified adsorbent.

2.2. X-ray diffraction, BET surface area, porosity and scanning electron microscope

X-ray diffraction (XRD) examination was used to analyze the phase composition of the BFS samples. The D8 Advance diffractometers (Bruker, United States) was used over the 10° - 70° 2θ range using Cu Kα radiation in the step-scan mode of 0.03^o. Four types of obtained BFS material were degassed at 150 ^{o}C for 13 hours under the vacuum condition. The Bruauer-Emmett-Teller (BET) method was used to measure the surface area by N_2 adsorption isotherm at 77 K using Autosorb iQ-C. The Barett-Joyner-Hanlenda (BJH) method served to calculate the total pore volume and average pore diameter. The surface morphology of the material was scanned by a Hitachi S3400 scanning electron microscope.

2.3. Batch adsorption experiments

The NH_4^+ solution was prepared by dissolving ammonium chloride (Merck, Germany) into the selected concentrations. The batch experiments were conducted by letting the fixed amount of adsorbents contacted with 50 mL of 20 mg/L NH_4^+ solutions for a certain period inside a 100 mL conical flask an electronic shaker at 120 rpm. The effect of acid modification on NH_4^+ adsorption capacity was studied at the experimental condition of pH 6, contact time of 4 hours, the adsorbent dosage of 10 g/L in 50 mL of NH_4^+ solution. The influence of pH was also investigated at similar conditions with pH variation from 2 to 11 adjusted by dropwise of HCl and NaOH. Various dosages of adsorbent were also tested from 0.2 g/L to 200 g/L to clarify the optimum amount of BFS material for NH_4^+ adsorption. The kinetic adsorption was conducted at pH 6 with an adsorbent dosage of 10 g/L and an ammonium concentration of 20 mg/L at different periods (after 15 to 180 minutes). The experiment was also conducted at different levels of NH_4^+ initial concentrations from 5 to 150 mg/L. The pH meter (HI 2211, Hanna Instrument, United States) was used for all pH measurements. NH_4^+ in the filtrates were measured by the International Organization for Standardization ISO 7150-1:1984 in Water quality – Determination of ammonium by manual spectrometric method (Reviewed and confirmed in 2017) [15] using the UV-VIS Double Beam PC Scanning Auto Cell (UVD-3200, Labomed Inc, United States). The amount of NH_4^+ adsorption at equilibrium, q_e (mg/g), was calculated as the equation below:

$$q_e = \frac{(C_o - C_e).V}{m} \tag{1}$$

where C_o is the initial concentration of NH_4^+ (mg/L), C_e is the equilibrium concentration of NH_4^+ (mg/L), V is the volume of the solution (L), and m is the adsorbent mass (g). The NH_4^+ removal efficiency (η) was calculated using the equation written as follows:

$$\eta\ (\%) = \frac{(C_o - C_e)}{C_o} \times 100. \tag{2}$$

The data was modeled using Langmuir (eq. 3) and Freundlich (eq.4) adsorption isotherms.

$$q_e = \frac{q_m K_L C_e}{1 + K_L C_e} \tag{3}$$

where q_m is the maximum NH_4^+ adsorption capacity (mg/g) and K_L is the Langmuir constant (L/mg) relating to the energy of adsorption.

$$q_e = K_F \times C_e^{1/n} \tag{4}$$

where K_F is the Freundlich constant $(mg/g)(L/mg)^{1/n}$ and n is the dimensionless Freundlich constant. For the kinetics of adsorption, the amount of NH_4^+ adsorbed at time t (q_t, mg/g) was calculated as follow:

$$q_t = \frac{(C_o - C_t)V}{m} \tag{5}$$

where C_t is the concentration of NH_4^+ at time t (mg/L). The data was modeled using pseudo-first order (eq.6) and pseudo-second order (eq.7) equations:

$$\frac{dq_t}{dt} = k_1(q_e - q_t) \tag{6}$$

where k_1 is the rate constant for pseudo-first order equation (1/h).

$$\frac{dq_t}{dt} = k_2(q_e - q_t)^2 \tag{7}$$

where k_2 is the rate constant for pseudo-second order equation (g/mg.h).

3. RESULTS AND DISCUSSION

3.1. Characteristics of the BFS adsorbents

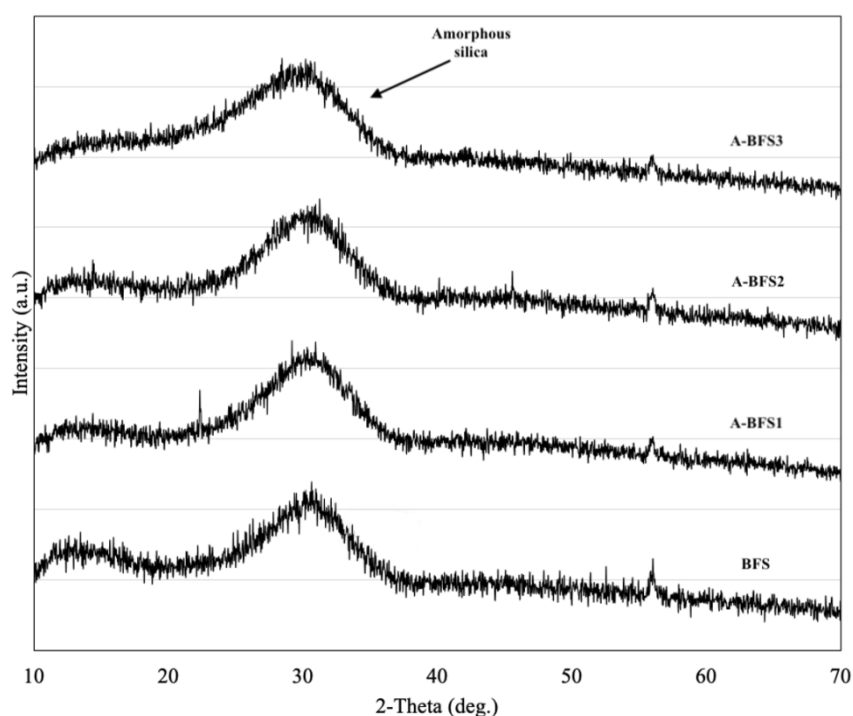The XRD analysis of the BFS materials is presented in Figure 1.

*Figure 1.* XRD pattern of BFS materials.

There were a low number of peaks at all four materials which indicated no crystalline phase was detected in the BFS materials. It describes that the effect of HNO_3 on the crystal structure of the BFS was negligible [16]. The common and most significant pattern was the single broad

612

amorphous peak at around 30°. This pattern is similar to the previous report for SiO_2 synthesized by sol-gel method [17]. It is reasonable since the composition of the BFS material comprises a high portion of SiO_2. This pattern of XRD was obtained as expected since the purpose of HNO_3 activation toward BFS was not to altering the primary crystal structure of BFS (which is represented as SiO_2). On the other hand, the acidic modification was expected to improve the surface area and the porosity of the BFS to have better solid-liquid interaction for the ammonium adsorption process. Therefore, the following BET and SEM results would be necessary to clarify the effect of HNO_3 modification.

The data of the surface area and pore volume of the BFS and A-BFS3 is presented in Table 1. According to the result, the acid modification has significantly enhanced the surface area and pore volume of the blast furnace slag. Specifically, the S_{BET} was increased 25.8 times (0.0895 to 2.3057 m^2/g) along with 10.4 times improved in V_P (from 0.000938 to 0.00972 cm^3/g) after the acidic activation with HNO_3 3M. Other studies that employed acidic activation using HNO_3 achieved a similar trend with activated carbon and sawdust biochar [10, 11].

Table 1. Steel compositions (wt.%) characterized by optical emission spectroscopy.

Sample	S_{BET} (m²/g)	V_P (cm³/g)
BFS	0.0895	0.000938
A-BFS3	2.3057	0.00972
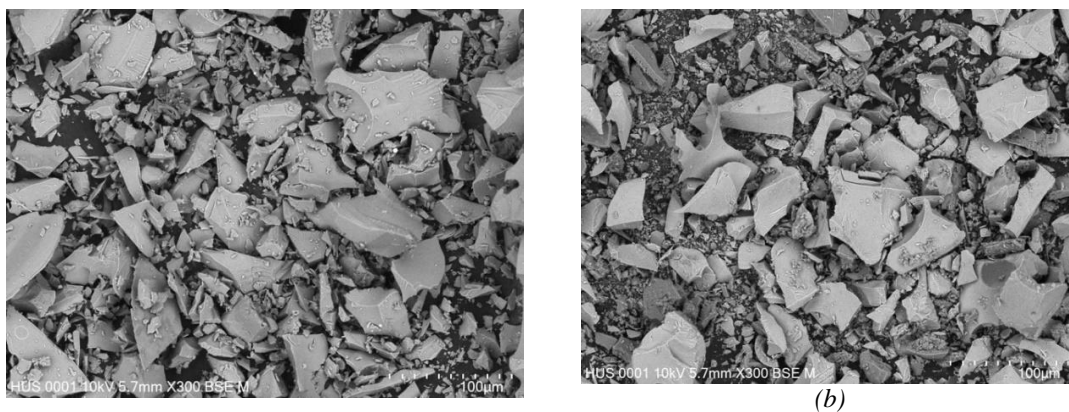
(a)
(b)
Figure 2. SEM photos of (a) BFS and (b) A-BFS3 adsorbent.

This phenomenon might be the reason for the wash-off of the contamination on the pore's surface of the BFS. The surface destruction by the acid to form new pores was also a possible answer for the increase of surface area. It can be observed that the material possessed a rough surface with much smaller particles after being modified with HNO_3 3M compared to its natural state (Figure 2).

3.2. Comparison of adsorption capacity between BFS materials

The comparison of NH_4^+ adsorption capacity between BFS materials was described in Figure 3. The role of HNO_3 modification was apparently expressed since the q value was increased at a higher HNO_3 concentration. The q value was approximately 10-time multiplied (0.07 mg/g to 0.76 mg/g) as a result of exposure of BFS with 0.5M HNO_3. The increasing rate of

q, however, slowed down when the concentrations of HNO_3 were used at higher concentrations of 1M and 3M. The adsorption capacity of the A-BFS2 and A-BFS3 were 0.98 and 1.29 mg/g, respectively. This trend could be the result of BFS surface oxidation which exhibited contamination removal and pore creation at the surface of the material. Vassileva *et al.* also found an improvement of NH_4^+ adsorption twice when the activated carbon was washed with HNO_3 acid [10]. Hereafter, the A-BFS3 adsorbent was chosen for the following investigations.
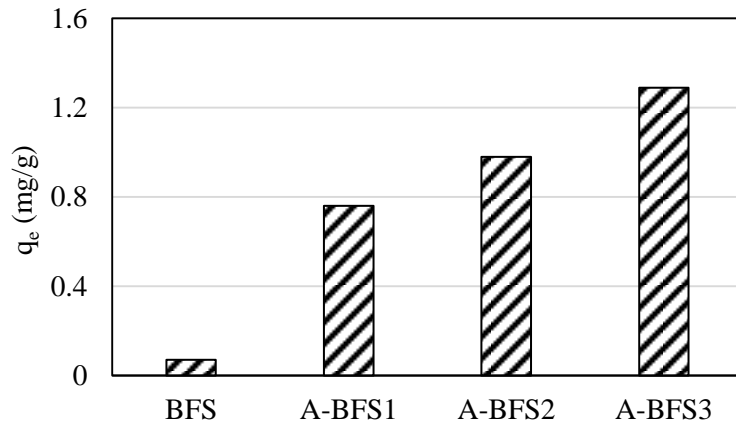

Figure 3. NH_4^+ adsorption capacity of BFS materials.

3.3. Effect of adsorbent dosage

The adsorbent dosage, which was measured at g/L, varied from 0.2 to 40 to see its influence on the NH_4^+ adsorption capacity and removal efficiency. According to Figure 4, the increase of A-BFS3 created two opposite trends of NH_4^+ adsorption capacity (q) and removal efficiency (η).
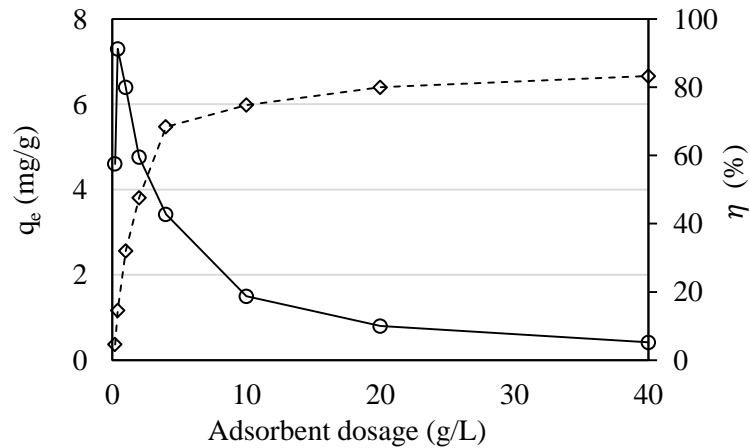

Figure 4. Effect of A-BFS3 dosage on its NH_4^+ adsorption capacity and removal efficiency
(○: adsorption capacity, ◊: removal efficiency).

The adsorption capacity went up sharply (4.6 mg/g to 7.30 mg/g) as the adsorbent dosage was slightly increased from 0.2 to 0.4 g/L. However, the q value started to tumble down as the dosage was higher than 0.4 g/L. Specifically, the q value dropped from 7.30 to 1.50 mg/g when

the dosage increase from 0.4 to 10 g/L. At the dosage higher than 10 g/L, the q value continued to go down but at a much slower pace and reached 0.42 mg/g at the dosage of 40 g/L. Conversely, the removal efficiency of NH_4^+ was recorded at an increasing trend as the adsorbent dosage went higher. The η value was boosted from only 4.6 % to 74.8 % of NH_4^+ removal as the dosage increased from 0.2 to 10 g/L. The η value then gradually increased by less than 10 % (74.8 % to 83.3 %) as the dosage reached 40 g/L. This could be explained by the equilibrium state of NH_4^+ solid-liquid transfer. When the system is presented with a limited amount of adsorbent, the excessive NH_4^+ ion would try to bound into the limited contacted surface between the adsorbent and liquid body. As the amount of adsorbent added to the solution was increased, there would be more contacting sites for NH_4^+ to take up leading to higher η value. However, the distribution of NH_4^+ on the adsorbent was scattered when a higher dosage was presented leading to lower q value. The state of NH_4^+ ion was subsequently reached the equilibrium state between in the liquid and in the adsorbent as the dosage passed 10 g/L. That was the reason for the slight change of q and η values at the dosage from 10 to 40 g/L.
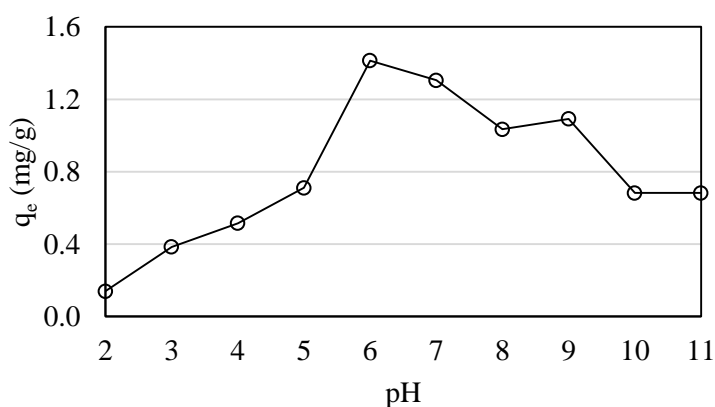
3.4. Effect of pH level

Figure 5. Effect of pH level on the NH_4^+ adsorption capacity of A-BFS3 dosage.

The influence of pH conditions on the NH_4^+ adsorption of A-BFS3 was illustrated in Figure 5. The result indicated that the optimum pH condition for NH_4^+ adsorption was around 6 to 7. At acidic condition, the existence of protons in the solution might be the competitive adsorbate with the NH_4^+ ion which resulted in limited adsorption capacity [1]. This phenomenon corresponded to the NH_4^+ adsorption on the surface of activated carbon, which possesses a minus zeta potential. The minus zeta potential surface allows the surface of the adsorbent to have higher cation exchange capacity, which exhibits better cation capture. Accordingly, the lowest q value was 0.14 mg/g at pH 2. The q value reached the peak of 1.41 mg/g at pH 6 then decreased at the higher pH. This finding was reasonable because NH_4^+ tends to shift to NH_3 gas at pH 9 and above. The NH_3 gas, which is a neutral compound, is not attracted to the surface of the adsorbent and is easily separated from the solution.

3.5. Effect of pH level

Initially, the adsorption of NH_4^+ on A-BFS3 was rapid. After 30 minutes, the adsorption capacity reached 1.14 mg/g as more than 60 % of NH_4^+ was removed. This value increased and remained around 1.33 to 1.36 mg/g in 1 to 3 following hours. The optimal contact time for NH_4^+

adsorption on A-BFS3 was 60 minutes according, which is an hour faster than that of the NH_4^+ adsorption on coconut shell biochar [18]. The experimental data was plotted together with the pseudo-first and -second order model with a pretty good agreement (R^2 = 0.933 - 0.999) (Table 2). The experimental data was closer to the prediction line of the pseudo-second order than the pseudo-first order for the A-BFS3 (Figure 6). It is suggested here that the adsorption mechanism of NH_4^+ onto A-BFS3 was mostly chemical.

Table 1. Steel compositions (wt.%) characterized by optical emission spectroscopy.

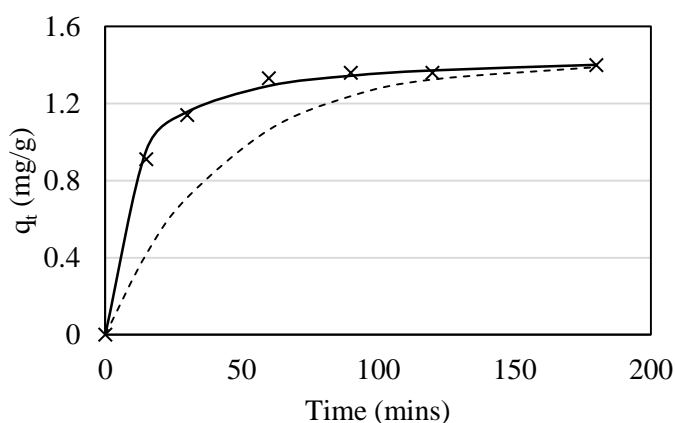| Adsorbent	Pseudo-first order (PFO)			Pseudo-second order (PSO)		
	q_e	k_1	R^2	q_e	k_2	R^2
	mg/g	min^{-1}		mg/g	g/mg.min	
A-BFS3	1.41	0.0234	0.933	1.463	0.086	0.999

Figure 6. Batch kinetic data for NH_4^+ adsorption on A-BFS3 (×: experimental data, dashed line: PFO prediction model, solid line: PSO prediction model).

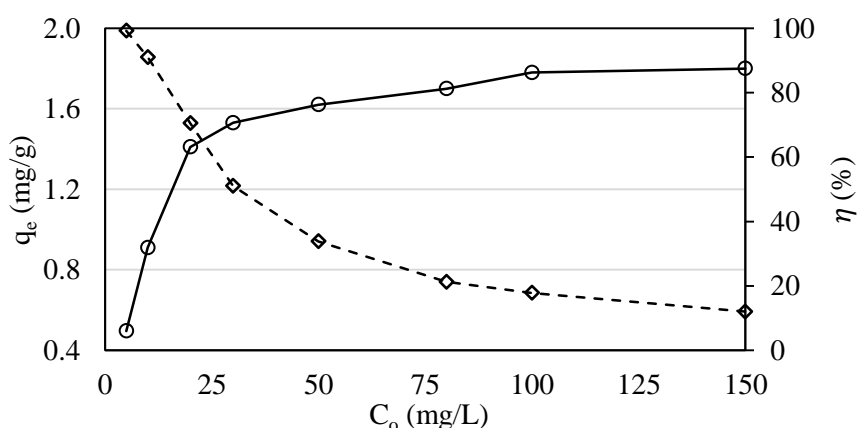## 3.6. Equilibrium batch NH_4^+ adsorption

Figure 7. Effect of NH_4^+ initial concentration on the adsorption capacity and removal efficiency (○: adsorption capacity, ◊: removal efficiency).

The effect of initial concentration on the NH_4^+ adsorption on A-BFS3 at pH 6 is presented in Figure 7. The increase of C_o resulted in higher adsorption capacity but lowering the removal efficiency. In particular, the q_e tripled (from 0.50 to 1.53 mg/g) while the η value dropped almost by half (99.2 to 51.0 %) as the C_o increased from 5 to 30 mg/L. At higher C_o from 30 to 150 mg/L, the improvement of q_e was insignificant when the increment was only 0.27 mg/g (from 1.53 to 1.80 mg/g). On the other hand, the η value continued to drop but a lower rate from 51% to 12% as the C_o increased to 150 mg/L. The increase of q_e was the result of the higher NH_4^+ content in the solution with a constant dosage of adsorbent. When the adsorption capacity reached the saturated state, the removal efficiency of NH_4^+ declined as a result.

The experimental data of equilibrium NH_4^+ adsorption isotherm are also presented in Figure 8 together with the Langmuir and Freundlich model. The experimental data are satisfactorily described by both Langmuir and Freundlich isotherm models with the coefficient of determination (R^2) of 0.99 and 0.91, respectively (Table 3).

Table 3. Langmuir and Freundlich model parameters and coefficient of determination (R^2) of the model's fits for NH_4^+ adsorption on A-BFS at pH 6.

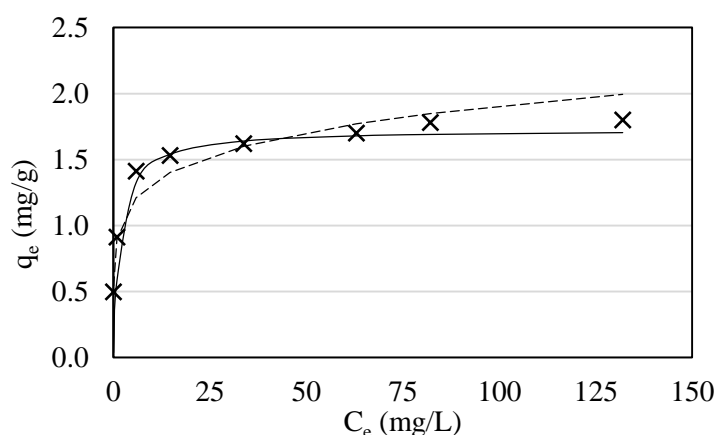| Adsorbent	Langmuir model			Freundlich model		
	q_m (mg/g)	K_L (L/mg)	R^2	K_F (mg/g)(L/mg)$^{1/n}$	n	R^2
A-BFS3	1.81 mg/g	0.52	0.99	0.91	6.22	0.96

Figure 8. Batch equilibrium data for NH_4^+ on A-BFS3 at pH 6 and the fit of experimental data (×) to Langmuir (solid line) and Freundlich (dashed line) models.

The result indicated that the Langmuir adsorption model fit was slightly better than the Freundlich model for A-BFS3, which explained 99 % of the data over 91 % by the Freundlich model. This expressed that the adsorption sites of NH_4^+ onto A-BFS3 are homogenous. The Langmuir adsorption capacity for A-BFS3 was 1.81 mg/g (Table 3). In the Langmuir model, the separation factor, R_L is calculated from the equation, $RL = 1/1(1+C_mK_L)$, where C_m is the maximum initial concentration of adsorbate. The R_L value describes the favorability of the adsorption process: unfavorable ($R_L > 1$), favorable ($0 < R_L < 1$), or irreversible ($R_L = 0$) [19]. The RL value for NH_4^+ adsorption on A-BFS3 was 0.013, which suggests that the process is favorable. The value of Freundlich constant $1/n$ was equal between 0.1 and 1 (0.16) which also described favorable adsorption and illustrated strong interaction between A-BF3 and NH_4^+ [19].

4. CONCLUSIONS

This study showed that the BFS material possesses the NH_4^+ adsorption ability and it can be enhanced with HNO_3 modification. The acid modification to BFS material improved the physical characteristic as the A-BFS3 achieved 25.7 times and 10.3 times improvements of surface area and pore volume, respectively. As the experimental condition was investigated, the optimal condition for NH_4^+ adsorption on A-BFS3 was pH 6, 60 minutes of contact time, 10 g/L of adsorbent dosage, and 20 mg/L of initial concentration. The Langmuir adsorption model ($R^2 = 0.99$) fitted the experimental data better than the Freundlich adsorption model ($R^2 = 0.96$) for the A-BFS3. The Langmuir maximum adsorption capacity of A-BFS3 at pH 6 was 1.81 mg/g. The results indicated that the BFS can be a promising adsorbent for NH_4^+ removal from groundwater or for the tertiary treatment process. However, further study on the column adsorption and on the effect of other ions like PO_4^{3-}, SO_4^{3-}, As, etc should be considered in the future.

CRediT authorship contribution statement. TMV: Data treatment, manuscript preparation. NTM: Supervision. NTPT: Formal analysis, Methodology. PLP: Formal analysis, Methodology. TVT: Supervision, Funding acquisition.

Declaration of competing interest. The authors declare that they have no known competing financial interests or personal relationships that could have appeared to influence the work reported in this paper.

REFERENCES

1. Karri R. R., Sahu J. N., and Chimmiri V. - Critical review of abatement of ammonia from wastewater, Journal of Molecular Liquids **261** (2018) 21-31. https://doi.org/10.1016/j.molliq.2018.03.120

2. Brian Oram P. - Ammonia in Groundwater, Runoff, Surface Water, Lakes and Streams. Available from: https://water-research.net/index.php/ammonia-in-groundwater-runoff-and-streams.

3. Bonsen E.-M., Schroeter S., Jacobs H., and Broekaert J. C. - Photocatalytic degradation of ammonia with t102 as photocatalyst in the laboratory and under the use of solar radiation, Chemosphere **35** (1997) 1431-1445. https://doi.org/10.1016/S0045-6535(97)00216-6

4. WHO - Guidelines for Drinking-water Quality, 4th Edition incorporating the first addendum 2017.

5. National technical regulation on drinking water quality - Ministry of Health: Viet Nam, 2009.

6. Liu H., Dong Y., Wang H., and Liu Y. - Ammonium adsorption from aqueous solutions by strawberry leaf powder: Equilibrium, kinetics and effects of coexisting ions, Desalination **263** (2010) 70-75. https://doi.org/10.1016/j.desal.2010.06.040

7. Halim A. A., Aziz H. A., Johari M. A. M., and Ariffin K. S. - Comparison study of ammonia and COD adsorption on zeolite, activated carbon and composite materials in landfill leachate treatment, Desalination **262** (2010) 31-35. https://doi.org/10.1016/j.desal.2010.05.036

8. De Gisi S., Lofrano G., Grassi M., and Notarnicola M. - Characteristics and adsorption capacities of low-cost sorbents for wastewater treatment: A review. Sustainable Materials and Technologies **9** (2016) 10-40. https://doi.org/10.1016/j.susmat.2016.06.002

9. Liu H., Dong Y., Liu Y., and Wang H. - Screening of novel low-cost adsorbents from agricultural residues to remove ammonia nitrogen from aqueous solution. Journal of Hazardous Materials **178** (2010) 1132-1136. https://doi.org/10.1016/j.jhazmat. 2010.01.117

10. Vassileva P., Tzvetkova P., and Nickolov R. - Removal of ammonium ions from aqueous solutions with coal-based activated carbons modified by oxidation, Fuel **88** (2009) 387-390. https://doi.org/10.1016/j.fuel.2008.08.016

11. Shang L., Xu H., Huang S., and Zhang Y. - Adsorption of Ammonium in Aqueous Solutions by the Modified Biochar and its Application as an Effective N-Fertilizer. Water, Air, & Soil Pollution **229** (2018) 320. 10.1007/s11270-018-3956-1

12. Xue Y., Wu S., and Zhou M. - Adsorption characterization of Cu(II) from aqueous solution onto basic oxygen furnace slag. Chemical Engineering Journal **231** (2013) 355-364. https://doi.org/10.1016/j.cej.2013.07.045

13. Kanel S. R., Choi H., Kim J. Y., Vigneswaran S., and Shim W. G. - Removal of Arsenic(III) from Groundwater using Low-Cost Industrial By-products-Blast Furnace Slag, Water Quality Research Journal **41** (2006) 130-139. 10.2166/wqrj.2006.015

14. Tran T. T. T., Yang C. M., Shen S., and Le M. H. - Research on survey and assessment of the conditions affecting arsenic adsorption and removal by steel slag in water. Vietnam Journal of Marine Science and Technology **32** (2015) 280-287. 10.15625/1859-3097/15/3/7224

15. ISO - Manual spectrometric method, in 7150-1:1984 Water quality - Determination of Ammonia Part 1, 1984.

16. Dai J., Wang Q., Xie C., Xue Y., Duan Y., and Cui X. - The Effect of Fineness on the Hydration Activity Index of Ground Granulated Blast Furnace Slag, Materials **12** (2019). 10.3390/ma12182984

17. Waseem M., Mustafa S., Naeem A., Shah K., Shah I., and Ihsan Ul H. - Synthesis and characterization of silica by sol-gel method, Journal of Pakistan Material Society **3** (2009) 19-21.

18. Boopathy R., Karthikeyan S., Mandal A. B., and Sekaran G. - Adsorption of ammonium ion by coconut shell-activated carbon from aqueous solution: kinetic, isotherm, and thermodynamic studies. Environmental Science and Pollution Research **20** (2013) 533-542. 10.1007/s11356-012-0911-3

19. Rusmin R., Sarkar B., Liu Y., McClure S., and Naidu R. - Structural evolution of chitosan–palygorskite composites and removal of aqueous lead by composite beads. Applied Surface Science **353** (2015) 363-375. https://doi.org/10.1016/j.apsusc. 2015.06.124